Detecting Quantum Critical Points Using Bipartite Fluctuations

Stephan Rachel,[1] Nicolas Laflorencie,[2] H. Francis Song,[1] and Karyn Le Hur[1]
[1]*Department of Physics, Yale University, New Haven, Connecticut 06520, USA*
[2]*Laboratoire de Physique Théorique, Université de Toulouse, UPS (IRSAMC), F-31062 Toulouse, France*
(Received 6 October 2011; published 12 March 2012)

We show that the concept of bipartite fluctuations $\mathcal{F}$ provides a very efficient tool to detect quantum phase transitions in strongly correlated systems. Using state-of-the-art numerical techniques complemented with analytical arguments, we investigate paradigmatic examples for both quantum spins and bosons. As compared to the von Neumann entanglement entropy, we observe that $\mathcal{F}$ allows us to find quantum critical points with much better accuracy in one dimension. We further demonstrate that $\mathcal{F}$ can be successfully applied to the detection of quantum criticality in higher dimensions with no prior knowledge of the universality class of the transition. Promising approaches to experimentally access fluctuations are discussed for quantum antiferromagnets and cold gases.

DOI: 10.1103/PhysRevLett.108.116401 PACS numbers: 05.30.Rt, 03.67.Mn, 05.70.Jk, 71.10.Pm

Quantum phase transitions [1] occur at zero temperature and are solely driven by quantum fluctuations. Hence, it is expected that a quantum phase transition should be manifested through the system's entanglement properties [2]. Identifying appropriate measures of entanglement is, however, a nontrivial task. An important tool to access and quantify the amount of entanglement between two subsets $\mathcal{A}$ and $\mathcal{B}$ of an interacting quantum system is the von Neumann entanglement entropy (EE). In one dimension (1D), conformal field theory and exact calculations have established the logarithmic scaling of the von Neumann entropy [3] for critical systems. For gapped systems, the EE saturates to a constant and thus obeys a strict area law (assuming a local Hamiltonian) [4]. In fact, EE can help to locate the quantum critical point (QCP) in some cases [5]; for more subtle situations (e.g., Kosterlitz-Thouless transitions), it was demonstrated recently that the EE failed to locate the QCP of the frustrated J_1-J_2 chain [6]. In higher dimensions, it was established that the gapless Heisenberg antiferromagnet on a square lattice obeys a strict area law [7,8], as also expected for a gapped phase. In such a situation, it is therefore unlikely that von Neumann EE will be a useful and practical tool to detect QCPs. Conversely, the valence bond entropy has been shown to be a powerful quantity to locate QCPs in any dimension, based on different scaling regimes, but it is restricted to SU(2)-invariant spin systems [6,9].

The aim of this Letter is to promote a general and more practical quantity to precisely locate QCPs for a larger variety of strongly correlated systems in any dimension d. Using the concept of *bipartite fluctuations* [10–12] $\mathcal{F}$ of particle number or magnetization in many-body quantum systems, we focus on systems where such U(1) charges $\mathcal{O}$ are *globally* conserved while they *locally* fluctuate within each subsystems. We define

$$\mathcal{F}_{\mathcal{A}} = \left\langle \left(\sum_{i\in\mathcal{A}} \mathcal{O}_i \right)^2 \right\rangle - \left\langle \sum_{i\in\mathcal{A}} \mathcal{O}_i \right\rangle^2, \qquad (1)$$

where the (globally) conserved quantity $\mathcal{O}$ can be the particle number n or the magnetization S^z and $\langle\cdot\rangle$ refers to the ground state at $T = 0$. $\mathcal{O}_i$ is defined for a subsystem $\mathcal{A}$ embedded in a larger one; see Fig. 1. For the special case that $\mathcal{A}$ is the total system, $\mathcal{F}_A$ is just the susceptibility (or compressibility, respectively) multiplied by the temperature. We show for various models, such as the spin-$\frac{1}{2}$ frustrated J_1-J_2 antiferromagnet in 1D, the Bose-Hubbard chain at unit filling, 2D coupled Heisenberg ladders, and Bose-condensed hard-core bosons on a square lattice, that $\mathcal{F}_{\mathcal{A}}$ provides a very efficient tool to accurately detect quantum criticality in the framework of quantum Monte Carlo (QMC) and density matrix renormalization group (DMRG) simulations on finite-size systems [13]. The key feature of the bipartite fluctuations is the distinct scaling behavior for gapless and gapfull phases in any dimension d [8,10,11], as summarized in Fig. 1: Within a subsystem of linear size L, $\mathcal{F}$ exhibits a strict area law for a disordered (gapped) ground state, $\mathcal{F}_{\text{gapped}} \propto L^{d-1}$, whereas for a (quasi)ordered gapless state *multiplicative* logarithmic corrections appear, $\mathcal{F}_{\text{gapless}} \propto L^{d-1} \ln L$, thus allowing one to precisely locate a QCP between two such regimes. The bipartite fluctuations give an alternative view of the correlation functions, since they are dominated by short-range fluctuations [11]. Experimentally, the concept of fluctuations has a very strong potential [12].

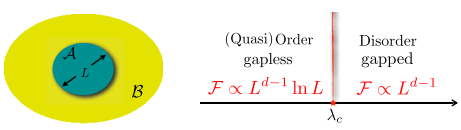

FIG. 1 (color online). For a d-dimensional system, the fluctuations $\mathcal{F}$ within subsystem $\mathcal{A}$ (of linear size L) with respect to $\mathcal{B}$ provide a precise estimate to locate a QCP at λ_c between gapless (quasi)ordered and gapped disordered phases with distinct scalings with L.

One-dimensional systems.—We now address 1D models, governed by Kosterlitz-Thouless–type quantum phase transitions usually difficult to precisely locate numerically. The first model we study is the frustrated spin-$\frac{1}{2}$ J_1-J_2 chain, governed by the Hamiltonian

$$\mathcal{H}(\lambda) = \sum_i (\mathbf{S}_i \cdot \mathbf{S}_{i+1} + \lambda \mathbf{S}_i \cdot \mathbf{S}_{i+2}), \tag{2}$$

where $J_2/J_1 \equiv \lambda \geq 0$. For $\lambda \leq \lambda_c$, this system has power-law critical correlations. At $\lambda_c \simeq 0.2412$, a Kosterlitz-Thouless transition into a dimerized phase occurs [14,15]. As mentioned above, the estimated value for the QCP using EE is not very precise compared to the established methods [14], because the prefactor of the leading term in the EE (i.e., the central charge c) is more or less insensitive to a change of λ close to the QCP [6]. Instead, we detect the transition by observing the behavior of $\mathcal{F}$ under variation of the control parameter λ, which triggers the quantum phase transition. The low-energy theory describing such a quasiordered state is the Tomonaga-Luttinger liquid [15], for which [11,12]

$$\mathcal{F}(L) = \frac{K}{\pi^2} \ln L + \text{cst}, \tag{3}$$

where $K = 1/2$ is the Luttinger liquid parameter of this SU(2) point. However, marginally irrelevant operators lead to sizable logarithmic corrections for K [16], when computed on finite-size systems. Interestingly, such corrections vanish precisely at λ_c, where K quickly reaches its asymptotic value of $1/2$. Thus we have a systematic method at hand to detect this phase transition. In Fig. 2, we have plotted the Luttinger parameter K extracted from finite-size DMRG calculations of Eq. (3) versus λ. For periodic boundary conditions (PBC) and $L = 100$, 150, 200, and 250, and after performing finite-size scaling, we obtain $\lambda_c = 0.2412(3)$ which agrees very well with the best estimates [14]. While there are a few other techniques available to find the QCP of the J_1-J_2 chain [6,14,17–19], our approach stands out through efficiency and simplicity.

Another interesting model is the Bose-Hubbard chain:

$$\mathcal{H} = -t \sum_{\langle ij \rangle} b_i^\dagger b_j + \frac{U}{2} \sum_i n_i(n_i - 1) - \sum_i \mu n_i, \tag{4}$$

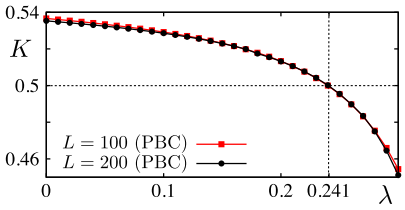

FIG. 2 (color online). Luttinger parameter K of the J_1-J_2 chain extracted via (3) versus $\lambda \equiv J_2/J_1$. Shown are DMRG data for $L = 100$ (red squares) and 200 (black dots) for PBC.

where t is the hopping amplitude, U the on-site repulsion, and μ the chemical potential. Away from half filling, we expect a superfluid-Mott transition triggered by $\lambda \equiv t/U$. The superfluid phase is a Luttinger liquid [20] with Luttinger parameter $K \geq 1$. For unit filling, the quantum phase transition from a superfluid to a Mott insulator is of Kosterlitz-Thouless type (like in the J_1-J_2 chain discussed above). The complete $(\mu, t/U)$ phase diagram was carefully investigated in Refs. [21–23]. Here we revisit the problem (restricted to unit filling) and show that we locate the transition with a better accuracy by virtue of the fluctuations. In the superfluid phase, the Green's function $G(r) = \langle b_r^\dagger b_0 \rangle \propto r^{-1/2K}$ decays as a power law. From Luttinger liquid theory, we know that the transition occurs for $K_c = 2$; see Ref. [24]. In Refs. [21,22], the Luttinger parameter K was extracted directly from $G(r)$, thus giving an estimate of the critical point $\lambda_c = 0.297 \pm 0.01$ [22]. The major advantages of our approach are that (i) the Luttinger parameter K can be extracted much more accurately from the fluctuations rather than the Green's function (see discussion in [13]) and (ii) the computational cost of $\mathcal{F}$ using DMRG (see Appendix C of Ref. [12]) is much lower as compared to the Green's function at large distances. We extract K from $\mathcal{F}$ for open boundary conditions with $L = 64$, 128, and 256 (the latter is shown in Fig. 3). By performing finite-size scaling, we obtain a much more precise estimate $\lambda_c = 0.2989(2)$, as compared to previous works [13].

Two dimensions.—Let us now move to 2D with a system of coupled spin-$\frac{1}{2}$ antiferromagnetic ladders, depicted in the inset in Fig. 4(a) and governed by the Hamiltonian

$$\mathcal{H} = \sum_{\text{ladd.}} \mathbf{S}_i \cdot \mathbf{S}_j + \sum_{\text{interladd.}} \lambda \mathbf{S}_i \cdot \mathbf{S}_j. \tag{5}$$

This model [25,26] displays a gapped valence bond solid (VBS) phase for small interladder coupling $\lambda < \lambda_c$ with $\lambda_c = 0.314\,07(5)$ [25], and a gapless Néel-ordered phase for $\lambda > \lambda_c$. Here we investigate the $T = 0$ fluctuations of the total magnetization in a region $\mathcal{A}$ of size $x \times y$ embedded in a periodic square lattice $L \times L$. We choose a

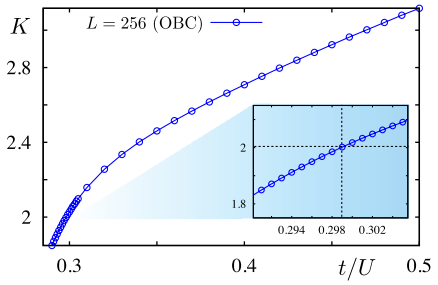

FIG. 3 (color online). Luttinger parameter K of the Bose-Hubbard chain extracted via (3) versus $\lambda \equiv t/U$ for $L = 256$ (unit filling) and open boundary conditions. We restricted the local boson occupation number to 4 [21,22]. Inset: Zoom close to the transition.

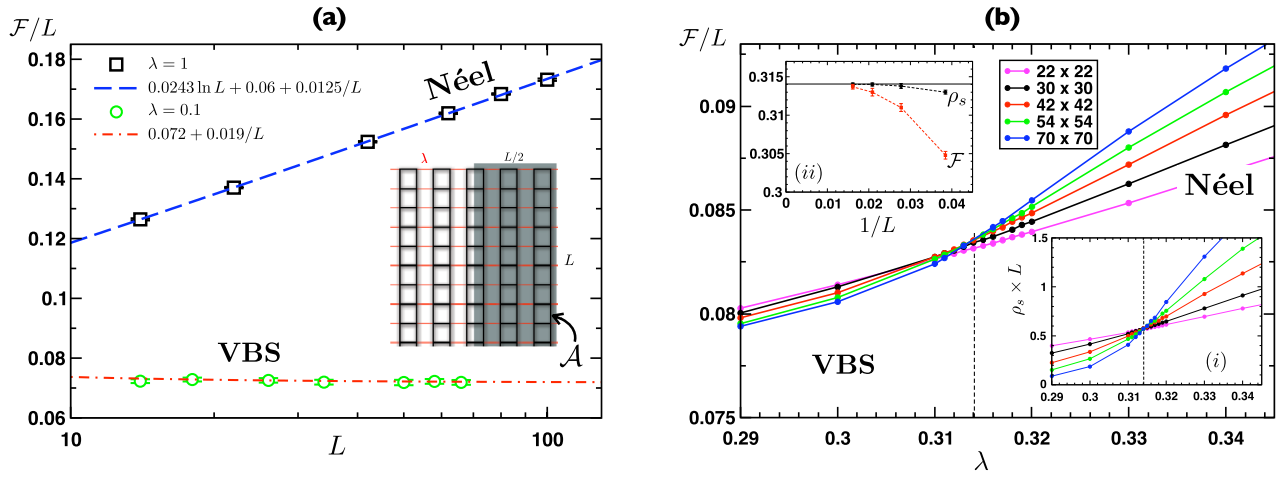

FIG. 4 (color online). Quantum Monte Carlo results for $T = 0$ fluctuations $\mathcal{F}$ of the total magnetization in a region $\mathcal{A}$ for 2D coupled spin-$\frac{1}{2}$ ladders [Eq. (5)], depicted in the inset in (a). Left (a): $\mathcal{F}/L$ increases logarithmically with L in the Néel regime (black squares $\lambda = 1$), whereas it saturates to a constant in the valence bond state (green circles $\lambda = 0.1$). Right (b): $\mathcal{F}/L$, plotted versus λ for various system sizes, displays a crossing point at λ_c. Insets: (i) Crossing of the stiffness $\rho_s \times L$ at λ_c for the same sizes; (ii) $1/L$ convergence of the crossing point for $\mathcal{F}$ (red squares) and ρ_s (black circles) to the critical value (horizontal black line) $\lambda_c = 0.314\,07$ [25].

subsystem $\mathcal{A}$ with $x = L/2$ and $y = L$ which contains an even number of sites. QMC results for the $T = 0$ [27] expectation of $\mathcal{F}(L/2)$ are shown in Fig. 4, with square lattice sizes up to $L \times L = 10^4$, for the isotropic square lattice $\lambda = 1$ (Néel) and for weakly coupled ladders with $\lambda = 0.1$ (VBS). In contrast with the entanglement (or Rényi) entropy which displays a strict area law in the Néel phase [7,8] (and presumably also in the VBS phase), the fluctuations follow a rather different scaling [8]:

$$\mathcal{F}(\ell) \sim \begin{cases} \alpha \ell \ln \ell + \beta \ell + \gamma & \text{(gapless Neél)}, \\ \beta' \ell + \gamma' & \text{(gapped VBS)}. \end{cases} \tag{6}$$

Therefore, $\mathcal{F}/\ell$ plotted for different sizes will display a crossing point at λ_c, as we indeed observe in Fig. 4(b), where the curves $\mathcal{F}(L/2)/L$ are plotted for various system sizes. The spin stiffness ρ_s, also known to be a useful quantity to locate a QCP, is shown in the right inset (i) in Fig. 4(b), where one sees a similar crossing for $\rho_s \times L^{d+z-2}$, with $z = 1$ and $d = 2$. As usual for such a technique, a drift of the crossing point is observed with L, as visible in the left inset (ii) in Fig. 4(b). Already known for a few other models [26,28], the crossing points obtained from the stiffness converge very rapidly with $1/L$ to the bulk value λ_c, whereas we found a slower convergence for the estimates obtained from $\mathcal{F}/L$. Despite such an effect (which may not be generic but model-dependent), we demonstrate here with this simple example that $\mathcal{F}$ is a very useful quantity to locate a QCP between ordered and disordered phases for $d > 1$.

One can get even more insight from the behavior of the coefficients α and β in Eq. (6) as a function of the interladder coupling λ (see Fig. 5). The prefactor α of the leading term $\sim L \ln L$ in the Néel phase vanishes at the critical point $\alpha \sim (\lambda - \lambda_c)^x$, with $x \simeq 0.7$ and $\lambda_c = 0.315(1)$, in good agreement with the value $0.314\,07(5)$ [25]. The area law term βL, displayed in Fig. 5(b), although certainly nonuniversal, exhibits a very interesting λ shape and passes through a maximum $\beta_c \simeq 0.0835$ at the critical coupling λ_c.

It is important to emphasize that, contrary to the stiffness, a prior knowledge of any critical exponent, such as the dynamical exponent z, is not necessary to precisely locate the QCP. Note also that we expect the valence bond entropy [9] to display similar crossing properties for such a SU(2) symmetric Hamiltonian [Eq. (5)]. In order to illustrate further the general character of this method, we focus now on a non-SU(2) model: hard-core bosons on the square lattice. Governed by the Hamiltonian

$$\mathcal{H} = -t \sum_{\langle ij \rangle} (b_i^\dagger b_j + \text{H.c.}) - \mu \sum_i b_i^\dagger b_i, \tag{7}$$

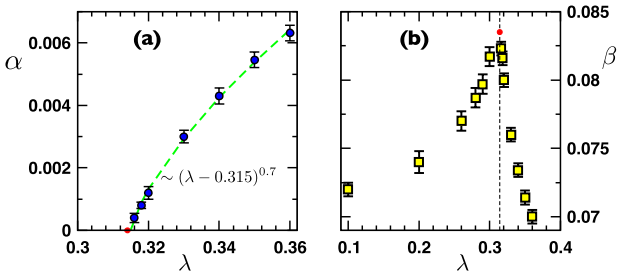

FIG. 5 (color online). Prefactors α and β from Eq. (6) for coupled Heisenberg ladders, extracted from the QMC data of Fig. 4 and plotted against λ. (a) The critical point is shown by a red circle, and the green curve is the power-law fit indicated on the plot. (b) The vertical dashed line signals the critical coupling λ_c, and the crossing point (red circle) is at $\beta_c \simeq 0.0835$.

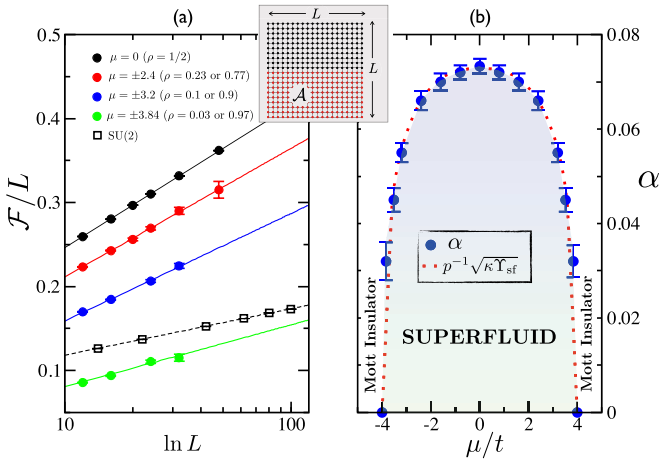

FIG. 6 (color online). QMC results for the fluctuations $\mathcal{F}$ of the particle number for hard-core bosons on square lattices of size $L \times L$, the subsystem $\mathcal{A}$ being half the lattice (see the inset). (a) $\mathcal{F}/L$ plotted against $\ln L$ for 4 representative fillings indicated on the plot and compared to the SU(2) Heisenberg model. (b) Prefactor α, obtained from fits to the form Eq. (6), shown over the entire regime versus μ/t together with $\sqrt{\kappa \Upsilon_{sf}}/p$ from QMC data, with $p = 3.2(1)$.

where b are hard-core boson operators, t the hopping integral, and μ the chemical potential, hard-core bosons on the square lattice [29] exhibit a particle-hole symmetric phase diagram with, at $T = 0$, a Bose-condensed superfluid state for $|\mu/t| < 4$ and trivial Mott insulating phases for $|\mu/t| > 4$, the transition between them being in the universality class of the dilute Bose gas with $z = 2$. The Bose-condensed [U(1)-broken-symmetry] state is expected to display for $\mathcal{F}$ (fluctuations of the particle number) a similar scaling as the one observed for SU(2)-broken Néel-ordered spins, whereas for the trivial Mott insulators we simply have $\mathcal{F}_{\text{Mott}} = 0$. In Fig. 6(a), $T = 0$ QMC results obtained for $\mathcal{F}$ are shown for 4 representative values of the chemical potential. The prefactor α of the $L \ln L$ term is plotted versus the chemical potential μ in the right panel of Fig. 6, where we observe a very interesting domelike shape in the superfluid regime. One can use an interesting analogy with quasi-one-dimensional systems where the Josephson-type interchain tunneling term will lock the superfluid phase difference between all chains. The low-energy (quasiordered) superfluid phase is described in terms of a single macroscopic 1D gapless mode. For a number of chains $N = L$, then we predict $\mathcal{F} = (KL/\pi^2) \ln L$. The logarithmic scaling of $\mathcal{F}$ is controlled by the Luttinger parameter K of the effective theory. In the hydrodynamic description of a Luttinger liquid, $K = \pi\sqrt{\kappa \Upsilon_{sf}}$, where κ is the compressibility and Υ_{sf} is the stiffness. This gives $\alpha = \sqrt{\kappa \Upsilon_{sf}}/\pi$. A similar quantum-hydrodynamic theory for interacting bosons is obtained in two dimensions by using the Gross-Pitaevskii approach. Comparing the prefactor α with $\sqrt{\kappa \Upsilon_{sf}}$ (obtained in the same QMC simulation), as shown in Fig. 6(b), gives a very good agreement. We find the following result for the entire superfluid regime: $\alpha(\mu) = \sqrt{\kappa \Upsilon_{sf}}/p$ with a coefficient $p \simeq 3.2(1)$. Scaling relations close to a QCP at λ_c predict $\Upsilon_{sf} \sim \xi^{2-d-z}$ and $\kappa \sim \xi^{z-d}$, thus leading to $\alpha \sim (\lambda - \lambda_c)^{\nu}$. This can be checked for Heisenberg ladders, as shown in Fig. 5(a), where the exponent $x \simeq 0.7$ is very close to $\nu = 0.709(6)$ of the 3D Heisenberg universality class [26].

Conclusion.—The concept of bipartite fluctuations of a (strongly correlated) quantum system has been shown for various paradigmatic condensed matter models to be an efficient, accurate, and rather general tool to detect quantum critical points by using state-of-the-art numerical techniques. In contrast to the von Neumann entropy, the fluctuations can be successfully used even in two spatial dimensions to find the critical point. Promising paths to directly measure the fluctuations have been proposed recently [12]; particularly interesting proposals are quantum magnets in an external magnetic field with Meissner screens (covering region $\mathcal{B}$) as well as direct measurement of $\mathcal{F}$ using single-atom microscopes [30]. A next step will be to test the usefulness of this tool for unconventional quantum criticality [31].

S. R. acknowledges support from DFG under Grant No. RA 1949/1-1 and partially from NSF DMR 0803200 and thanks P. Schmitteckert for use of his DMRG code. H. F. S. and K. L. H. acknowledge support from NSF DMR 0803200 and from the Yale Center for Quantum Information Physics through NSFR DMR-0653377.

[1] M. Vojta, Rep. Prog. Phys. **66**, 2069 (2003).
[2] A. Osterloh, L. Amico, G. Falci, and R. Fazio, Nature (London) **416**, 608 (2002); L. Amico, R. Fazio, A. Osterloh, and V. Vedral, Rev. Mod. Phys. **80**, 517 (2008).
[3] C. Holzhey, F. Larsen, and F. Wilczek, Nucl. Phys. **B424**, 443 (1994); G. Vidal, J. I. Latorre, E. Rico, and A. Kitaev, Phys. Rev. Lett. **90**, 227902 (2003); P. Calabrese and J. Cardy, J. Stat. Mech. (2004) P06002.
[4] M. B. Hastings, J. Stat. Mech. (2007) P08024; J. Eisert, M. Cramer, and M. B. Plenio, Rev. Mod. Phys. **82**, 277 (2010).
[5] M. Dalmonte, E. Ercolessi, and L. Taddia, Phys. Rev. B **84**, 085110 (2011).
[6] F. Alet, I. P. McCulloch, S. Capponi, and M. Mambrini, Phys. Rev. B **82**, 094452 (2010).
[7] A. B. Kallin, I. Gonzalez, M. B. Hastings, and R. G. Melko, Phys. Rev. Lett. **103**, 117203 (2009); M. B. Hastings, I. Gonzalez, A. B. Kallin, and R. G. Melko, *ibid.* **104**, 157201 (2010).
[8] H. F. Song, N. Laflorencie, S. Rachel, and K. Le Hur, Phys. Rev. B **83**, 224410 (2011).
[9] F. Alet, S. Capponi, N. Laflorencie, and M. Mambrini, Phys. Rev. Lett. **99**, 117204 (2007).
[10] D. Gioev and I. Klich, Phys. Rev. Lett. **96**, 100503 (2006).

[11] H. F. Song, S. Rachel, and K. Le Hur, Phys. Rev. B **82**, 012405 (2010).
[12] H. F. Song, S. Rachel, C. Flindt, I. Klich, N. Laflorencie, and K. Le Hur, Phys. Rev. B **85**, 035409 (2012).
[13] See Supplemental Material at http://link.aps.org/supplemental/10.1103/PhysRevLett.108.116401 for comparison of the presented approach to other methods.
[14] K. Okamoto and K. Nomura, Phys. Lett. A **169**, 433 (1992); S. Eggert, Phys. Rev. B **54**, R9612 (1996).
[15] F. D. M. Haldane, Phys. Rev. B **25**, 4925 (1982).
[16] N. Laflorencie, S. Capponi, and E. S. Sørensen, Eur. Phys. J. B **24**, 77 (2001).
[17] R. Thomale, D. P. Arovas, and B. A. Bernevig, Phys. Rev. Lett. **105**, 116805 (2010).
[18] M. Roncaglia *et al.*, Phys. Rev. B **77**, 155413 (2008).
[19] M. Thesberg and E. S. Sørensen, Phys. Rev. B **84**, 224435 (2011).
[20] T. Giamarchi, *Quantum Physics in One Dimension* (Oxford University, Oxford, 2004).
[21] T. D. Kühner and H. Monien, Phys. Rev. B **58**, R14 741 (1998).
[22] T. D. Kühner, S. R. White, and H. Monien, Phys. Rev. B **61**, 12 474 (2000).
[23] V. A. Kashurnikov, A. V. Krasavin, and B. V. Svistunov, JETP Lett. **64**, 99 (1996); S. Ejima, H. Fehske, and F. Gebhard, Europhys. Lett. **93**, 30 002 (2011); I. Danshita and A. Polkovnikov, Phys. Rev. A **84**, 063637 (2011).
[24] T. Giamarchi and A. J. Millis, Phys. Rev. B **46**, 9325 (1992).
[25] M. Matsumoto, C. Yasuda, S. Todo, and H. Takayama, Phys. Rev. B **65**, 014407 (2001).
[26] S. Wenzel, L. Bogacz, and W. Janke, Phys. Rev. Lett. **101**, 127202 (2008).
[27] To overcome finite-T effects and get ground-state estimates, QMC simulations were performed at $\beta/L = 10$ J.
[28] L. Wang, K. Beach, and A. Sandvik, Phys. Rev. B **73**, 014431 (2006).
[29] K. Bernardet, G. G. Batrouni, J.-L. Meunier, G. Schmid, M. Troyer, and A. Dorneich, Phys. Rev. B **65**, 104519 (2002); T. Coletta, N. Laflorencie, and F. Mila, arXiv:1112.5586.
[30] W. S. Bakr *et al.*, Science **329**, 547 (2010); J. F. Sherson *et al.*, Nature (London) **467**, 68 (2010).
[31] A. W. Sandvik, Phys. Rev. Lett. **98**, 227202 (2007).